

Direct measurement of double-K fracture parameters and fracture energy using wedge-splitting test on compact tension specimens with different size

S. Xu, D.Bu, H.Gao, S.Yin, Y.Liu

Department of Civil Engineering, Dalian University of Technology, Dalian, China

ABSTRACT: Wedge-splitting on compact tension specimen testing method is a technique which carries out fracture tests by combining the compact tension geometry configuration with the wedge-splitting loading pattern in wedge splitting testing method. Usually for wedge-splitting specimens especially for ones with larger size, the vertical component of load applied on specimen is not collinear with the supporting reaction force, thereby producing the additional moment which influences the measured value of fracture parameters. The present method can remove such impact, and lower the stiffness required for machine. A total of 36 specimens with different sizes of which the maximum size is $1250\text{mm}\times 1200\text{mm}\times 200\text{mm}$ are prepared to examine double-K fracture parameters and fracture energy. The experimental results show that the used fracture testing method is easy and stable. Moreover, the measured double-K fracture parameters K_{Ic}^{ini} , K_{Ic}^{un} are independent of specimens' size, similar to which the determined fracture energy has no size-effect within the testing range.

1 INSTRUCTIONS

Three-point bending test (TPBT) on notched beams, compact tension test (CT-test) and wedge splitting test (WS-test) have been widely used to determine the fracture parameters of cementitious materials (Swartz & Refai 1987, Xu & Zhao 1991, Xu et al. 1991, Ratanalert & Wecharatana 1989, Wittmann et al. 1990, Brühwiler & Wittmann 1990, Zhao et al. 1991, Kim et al. 1992, Mihashi et al. 1994, Wang & Wu 1992, Zhu 1997). Three-point bending test is easier to perform and has been recommended to determine the fracture energy of mortar and concrete by RILEM Technical Committee 50-FMC. CT specimens are often used to study the fracture toughness and fracture energy of plain concrete materials (Xu & Zhao 1991, Xu et al. 1991, Ratanalert & Wecharatana 1989, Wittmann et al., 1990). WS-test proposed by Hillemeier & Hilsdorf, (Hillemeier & Hilsdorf 1977) and then used by Bruhwiler & Wittmann (Brühwiler & Wittmann 1990) weakens the stiffness requirements compared to with TPBT, besides it is easier to carry out than CT-test. Especially it can be used to study the fracture behavior of the material in an existing structure by drilling cores. Therefore, the wedge splitting specimens were utilized to investigate the fracture toughness and fracture energy and other fracture parameters for concrete materials by many researchers (Hillemeier & Hilsdorf 1977, Brühwiler & Wittmann 1990, Zhao et al. 1991, Kim et al. 1992, Mihashi et al. 1994, Wang & Wu 1992, Zhu 1997).

In order to describe the complete fracture process of concrete including cracking initiation, steady crack propagation and unsteady crack propagation, a double-K crack propagation criterion was proposed in our prior work (Xu & Reinhardt 1999a). The determination and analytical evaluation of K_{Ic}^{ini} and K_{Ic}^{un} using three-point bending notched beams, compact tension specimens and wedge splitting specimens were conducted (Xu and Reinhardt 1999b,c). Due to the complexity of compact tension specimen test, three-point bending notched beams and wedge splitting specimens were frequently used to determine the fracture parameters for concrete.

Theoretically, the minimum specimen depth required for no size-effect double-K fracture parameters determined using the two test methods should be uniform. However, it was found that double-K fracture parameters were independent of specimen size when the depths of three-point bending notched beams exceed 200mm while the depths of wedge splitting specimens exceed 300mm or 400mm. After analyzing plentiful testing results, we think that following reasons might contribute to the differences. First, there is no exact formula to evaluate stress intensity factor K_I for the wedge splitting specimens. Because the specimen geometry and the loading condition of the wedge splitting specimen are similar to those of the CT-specimen, the formula for the wedge splitting tests are the same as that proposed by Tada for the corresponding standard compact tension geometry. (Hillemeier & Hilsdorf 1977, Brühwiler & Wittmann 1990, Zhao et al. 1991, Kim et al. 1992, Mihashi et al. 1994, Wang and Wu 1992, Zhu,

1997, Xu & Reinhardt 1999a, b,c, Refai & Swartz, 1987, ASTM Standard E399-72 1972, Murakami 1987). Second, the measured values of fracture parameters are influenced by the additional moment caused by the non-collinear vertical forces. Usually there is only one loading device for all the wedge splitting specimens with different dimensions, thus the vertical component of load applied on specimen especially for ones with larger size is not collinear with the supporting reaction force, thereby producing the additional moment which influences the distribution of stress nearby the crack tip. In order to eliminate the influence of the additional moment on the true values of double- K fracture parameters and G_F , the vertical component of the applied load should be counteracted with the dead weight and the support force, that is, it is desired that loading devices with different dimensions should be used for different specimen dimensions. Considering the advantages of the two specimen geometries and in order to provide sufficient experimental data to support testing specification, to have better understanding of size-effect on double- K fracture parameters and fracture energy G_F together with further identifying the minimum specimen depth required for no size-effect double- K fracture parameters to make practical engineering application more convenient, a new testing approach, i.e., wedge-splitting test on compact tension specimen is attempted.

2 EXPERIMENTAL INVESTIGATION

2.1 Test set-up

Compact tension specimen and wedge splitting loading manner are used in wedge-splitting test on compact tension specimen. The set-up is present in (Figs 1-2). The loading devices compose of wedge loading device rollers and steel axials; Where wedge loading device is produced by jointing a twice H-beam and two identical wedges. The shapes of the wedges and rollers are the same as ones in the wedge loaded CT-specimens tests and the WS-tests. A specimen is prepared with a groove and a notch. Besides, the two loading holes and the double linear supports on the specimen are both collinear with the quarter of the specimen length. Then the wedge loading device equipped with rollers and steel axials is placed on the specimen. The top of the wedge loading device is fixed with the upper plate of the testing machine. Since the rollers are on the quarter of the specimen length, the designed loading devices should be adjusted to different specimen sizes.

During the test, the load P applies to the specimen via the wedge device, rollers and the steel axles in turn. The vertical components ($P/2$) of the force acting on the rollers counteract with the dead weight and the support force. Hence there is no additive

bending moment at the crack tip and only the splitting force (P_h) which transforms from the horizontal components influence the distribution of stress. Moreover, the formula to evaluate stress intensity factor K_I for CT-specimen can be used directly. So the real values of fracture parameters can be obtained.

The main advantage of the test is the use of the compact tension specimen whose rollers are on the quarter of the specimen length. Hillemeier and Hilsdorf had performed the wedge loaded CT-specimens' test in 1970s(Hillemeier & Hilsdorf,

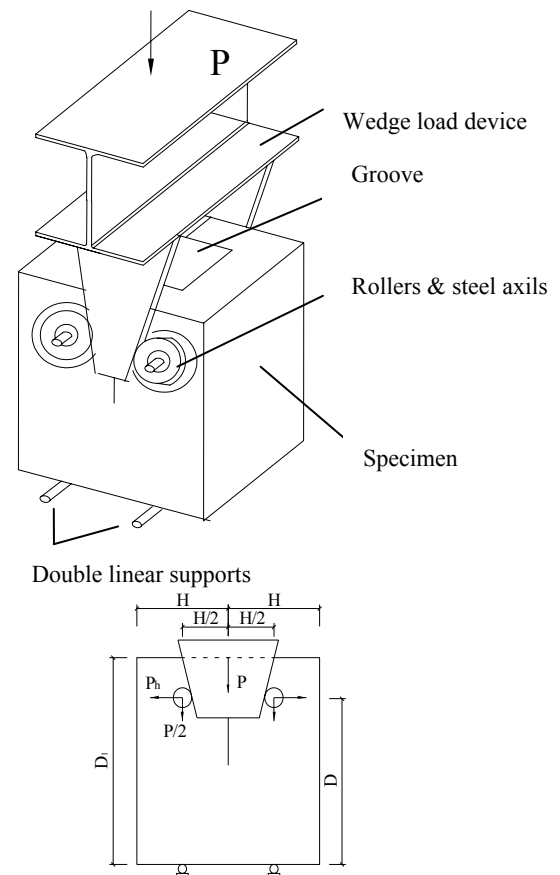


Figure 1. Configuration of the wedge-splitting test on compact tension specimens and loading devices and specimen dimension and the distribution of forces.

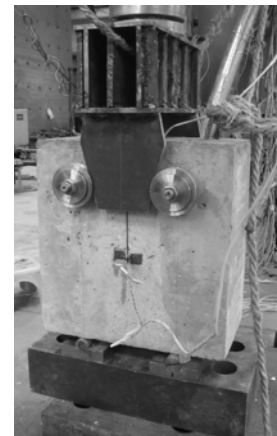


Figure 2. Wedge-splitting test on compact tension specimens and loading devices.

1977), but there still was additive bending moment for the CT-specimens designed according to ASTM E399/72 because the vertical load components acted

on the specimen were non-collinear with the dead weight and support forces. For the applied load acting on the specimen directly by wedges, rollers and axials the load-passing plates used in the WS-tests are unnecessary.

2.2 Determination of crack initiation

In our prior investigation for the determination of starting point of stable crack propagation and the critical unstable point of crack propagation four investigating techniques had been studied, i.e., laser speckle interferometry, acoustic emission, photoelastic coating and strain gauges. In this experiment, strain gauges were used to monitor crack initiation and development. As shown in Fig. 3, some electric strain resistance gauges are arranged along the direction of the fracture ligament. The two electric strain resistance gauges which were symmetrically arranged at the both sides of the ligament and the other two identical strain resistance gauges make up a full-bridge electro circuit. Each an electric strain resistance gauge which was arranged along the direction of the fracture ligament adding one strain gauge compensator composes a half-bridge electro circuit. specimen dimension. The notch was cast using a greased steel plate with a thickness of 3mm. The two holes for steel axials should be exactly on All the strain gauges resistance gauges should be arranged on the same concrete material. The strain gauges at the notch tip were used to monitor crack initiation, the rest were all for investigating the crack development.

Energy is stored in the specimen at the beginning of the application of the load and the value of the first pair of strain grow with the applied load lineally. Once maximum strain is reached, the stored energy is released and the value of strain turns to lessen (as seen in Fig. 4). The turning point can be taken as the initial point of stable crack propagation. The load values corresponding to the crack initiation are just initial cracking load P_{ini} . The results obtained from this method can be in agreement with the investigated results which corresponding to the starting point of nonlinear segment on a measured P - $CMOD$ curve or P - $CTOD$ curve. Similarly, other strain gauges present the same characteristic which implies that the crack passes through them. As a consequence, the process of the crack propagation can be investigated.

2.3 Specimen and test procedure

A total of 36 specimens of different heights D (200mm, 300mm, 400mm, 600mm, 800mm, 1000mm) were tested. The initial crack/depth ratio a_0/d was 0.4. The specimens were produced with the same mix proportions of 1:1.87:3.36:0.57 (cement: sand: coarse aggregate: water). The maximum size of the coarse aggregate was 25mm. All CT-specimens were cast in one day and were cured by

sealing them up with plastic membranes. A CT-specimen was prepared with a groove, a notch and two holes. The size of the groove which was big

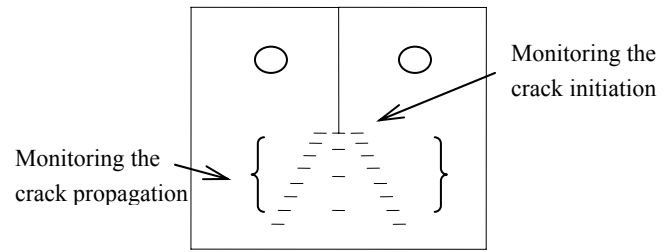


Figure 3. Distribution of the measuring points by using electronic resistant strain gauges.

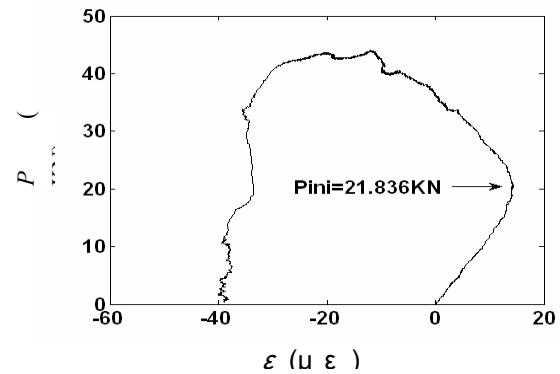


Figure 4. The P - ϵ curve of CT1000-1.

enough for fixing a strain gauge changed with the quarter line of the specimen length. The experiments were carried out after 170 days to 210 days. The measured cube compressive strength is 53.3MPa. The sizes of the specimens are presented in Table 1.

Experiments were carried out using a servo hydraulic closed-loop testing machine under displacement control. In the tests, the applied load P , the crack mouth opening displacement ($CMOD$), the crack tip opening displacement ($CTOD$) are measured. Electronic resistant strain gauges were used to measure the crack initiation and crack propagation.

All the information was collected by a computer-controlled 16 channel data-acquisition system.

Table1. Test specimen dimensions.

| Nos. of specimen | $2H \times D \times B$ | a_0 | D_1 |
|------------------|------------------------|-------|-------|
| | mm×mm×mm | mm | mm |
| CT200 | 240×200×200 | 80 | 250 |
| CT300 | 360×300×200 | 120 | 375 |
| CT400 | 480×400×200 | 160 | 500 |
| CT600 | 720×600×200 | 240 | 750 |
| CT800 | 960×800×200 | 320 | 1000 |
| CT1000 | 1200×1000×200 | 400 | 1250 |

3 DETERMINATION OF DOUBLE-K FRACTURE PARAMETERS USING WEDGE-SPLITTING TEST ON COMPACT TENSION SPECIMENS WITH DIFFERENT SIZES

In the researches, the stable crack propagation has been widely noted while the crack initiation has not been considered in the evaluation of crack propaga-

tion in concrete structures. In fact, for some concrete structures in some special cases the exact evaluation of the crack initiation cannot be neglected. Double- K criterion predicts that there exist three different states, i.e., crack initiation, stable crack propagation and unstable fracture in the fracture process in concrete structures. The double- K criterion consists of two size-independent parameters. One is the initial cracking toughness K_{lc}^{ini} , and the other is the unstable fracture toughness K_{lc}^{un} . The fracture parameters are required to be measurable in the experiments and should be only dependent on the material properties.

The initial toughness K_{lc}^{ini} is the initial cracking stress intensity factor created at the initial crack tip by the initial cracking load P_{ini} . Until the applied load arrives at P_{ini} , the concrete is at the linear elastic state, so the K_{lc}^{ini} can be directly evaluated by the initial cracking load P_{ini} , and the precast crack length a_0 , using a formula of LEFM. Similarly, the unstable fracture toughness K_{lc}^{un} can be obtained inserting the maximum load, P_{max} , and the effective crack length, a_c , into the same formula of LEFM. This approach is the same as that in the prior literature (Xu and Reinhardt 1999a,b,c). The measured P_{ini} , a_0 , P_{max} , a_c and the corresponding values of double- K fracture parameters are presented in Table 2. The P - $CMOD$ curves and P - $CTOD$ curves measured from the two specimens are shown in Fig. 5.

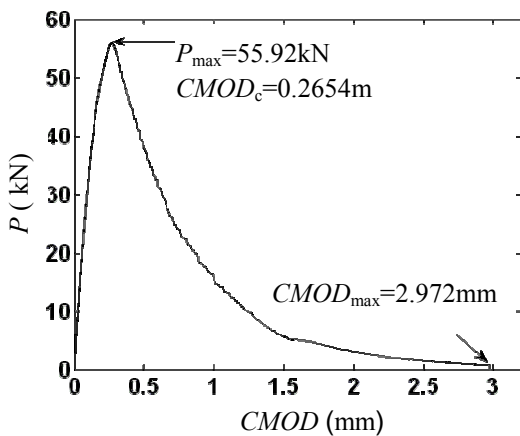


Figure 5. (a) the P - $CMOD$ curve of CT1000-3.

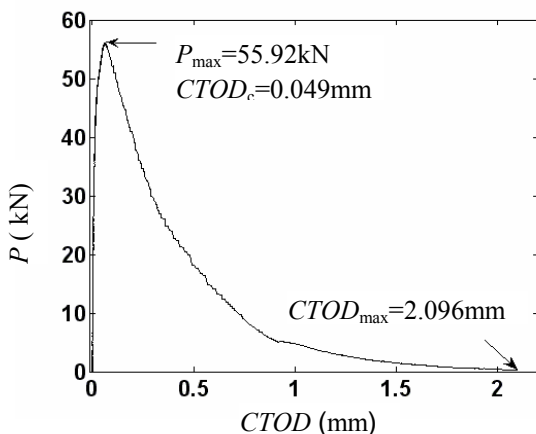


Figure 5.(b) the P - $CTOD$ curve of CT1000-3.

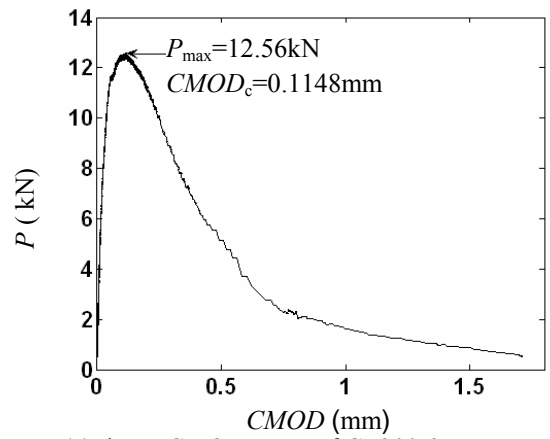


Figure 5. (c) the P - $CMOD$ curve of CT300-3.

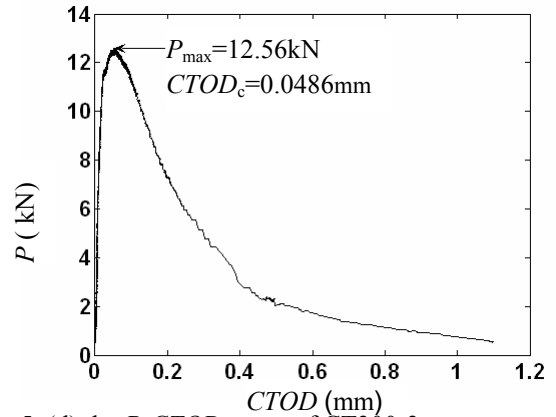


Figure 5. (d) the P - $CTOD$ curve of CT300-3.

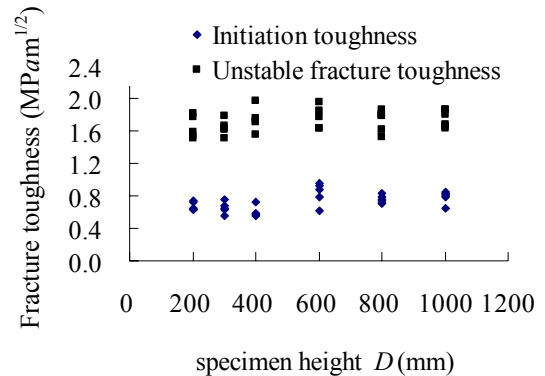


Figure 6. The plots of the Double- K fracture parameters vs. specimen height.

The plots of the double- K fracture parameters versus the specimen height are shown in Fig. 6. It can be seen that the values of initiation toughness K_{lc}^{ini} and unstable fracture toughness K_{lc}^{un} are independent of the specimen height in the tested ranges.

4 DETERMINATION OF FRACTURE ENERGY USING WEDGE- SPLITTING TEST ON COMPACT TENSION SPECIMENS WITH DIFFERENT SIZES

The specific fracture energy G_F is a useful fracture parameter for analyzing the fracture behavior of materials. A test for measuring the fracture energy is

Table2. Double-K fracture parameters directly measured from experiments.

| Nos. of specimens | a_0 (mm) | P_{ini} (N) | P_{max} (N) | a_c (mm) | $CMOD_c$ (μ m) | E (GPa) | K_{lc}^{ini} (MPam ^{1/2}) | K_{lc}^{un} (MPam ^{1/2}) |
|-------------------|------------|---------------|---------------|------------|---------------------|-----------|---------------------------------------|--------------------------------------|
| CT 200-1 | 80 | 7856 | 10023 | 120.4 | 89.80 | 35.90 | 0.635 | 1.593 |
| CT 200-2 | 80 | 7816 | 10690 | 111.9 | 89.40 | 31.85 | 0.656 | 1.617 |
| CT 200-3 | 80 | 7657 | 9622 | 118.9 | 88.80 | 35.05 | 0.662 | 1.647 |
| CT 200-4 | 80 | 9134 | 10609 | 122.7 | 97.50 | 38.92 | 0.753 | 1.859 |
| CT 200-6 | 80 | 8657 | 10938 | 119.5 | 99.47 | 35.97 | 0.725 | 1.764 |
| Aver. | 80 | 8224 | 10376 | 118.7 | 92.99 | 35.54 | 0.686 | 1.696 |
| CT 300-1 | 120 | 9975 | 15330 | 170.7 | 114.81 | 34.41 | 0.675 | 1.819 |
| CT 300-2 | 120 | 10452 | 14788 | 171.0 | 101.36 | 38.39 | 0.711 | 1.712 |
| CT 300-3 | 120 | 8214 | 12561 | 189.6 | 114.81 | 41.80 | 0.456 | 1.819 |
| CT 300-4 | 120 | 11316 | 15129 | 160.1 | 119.86 | 27.15 | 0.740 | 1.486 |
| CT 300-5 | 120 | 8930 | 12068 | 183.4 | 123.70 | 28.31 | 0.614 | 1.611 |
| Aver. | 120 | 9777 | 13975 | 175.0 | 114.91 | 34.01 | 0.639 | 1.690 |
| CT 400-1 | 160 | 9957 | 19584 | 217.8 | 124.30 | 36.22 | 0.562 | 1.707 |
| CT 400-2 | 160 | 10338 | 18979 | 208.6 | 112.50 | 34.87 | 0.583 | 1.536 |
| CT 400-3 | 160 | 12202 | 22467 | 216.3 | 140.60 | 36.74 | 0.702 | 1.928 |
| CT 400-6 | 160 | 9816 | 18289 | 228.1 | 146.80 | 24.34 | 0.546 | 1.742 |
| Aver. | 160 | 10418 | 19830 | 217.7 | 131.05 | 33.04 | 0.598 | 1.728 |
| CT 600-1 | 240 | 20473 | 26416 | 306.0 | 144.93 | 33.92 | 0.928 | 1.651 |
| CT 600-2 | 240 | 18700 | 28131 | 330.7 | 192.54 | 31.21 | 0.788 | 1.850 |
| CT 600-3 | 240 | 13751 | 27208 | 305.8 | 145.06 | 34.04 | 0.620 | 1.635 |
| CT 600-4 | 240 | 22359 | 29120 | 315.5 | 176.50 | 31.21 | 0.960 | 1.776 |
| CT 600-6 | 240 | 20064 | 30227 | 321.5 | 179.40 | 34.49 | 0.876 | 1.959 |
| Aver. | 240 | 190.69 | 28221 | 315.9 | 167.69 | 32.97 | 0.834 | 1.774 |
| CT 800-1 | 320 | 22109 | 34696 | 436.2 | 218.96 | 30.23 | 0.751 | 1.783 |
| CT 800-2 | 320 | 22245 | 34996 | 441.0 | 225.00 | 29.88 | 0.739 | 1.790 |
| CT 800-3 | 320 | 20655 | 33728 | 394.6 | 154.39 | 33.33 | 0.713 | 1.524 |
| CT 800-4 | 320 | 20415 | 33968 | 414.7 | 176.50 | 32.28 | 0.713 | 1.619 |
| CT 800-5 | 320 | 21973 | 37835 | 404.7 | 196.91 | 31.29 | 0.792 | 1.797 |
| CT 800-6 | 320 | 23404 | 34255 | 437.7 | 195.37 | 35.37 | 0.823 | 1.864 |
| Aver. | 320 | 21800 | 34193 | 421.5 | 194.52 | 32.06 | 0.755 | 1.730 |
| CT 1000-1 | 400 | 21836 | 43580 | 497.9 | 218.82 | 29.06 | 0.644 | 1.670 |
| CT 1000-2 | 400 | 28539 | 46631 | 472.4 | 205.26 | 29.28 | 0.843 | 1.661 |
| CT 1000-3 | 400 | 29948 | 55918 | 483.1 | 265.38 | 25.77 | 0.791 | 1.860 |
| CT 1000-4 | 400 | 27290 | 48169 | 479.6 | 214.15 | 30.63 | 0.815 | 1.794 |
| CT 1000-5 | 400 | 28448 | 45522 | 478.3 | 206.00 | 29.05 | 0.823 | 1.616 |
| CT 1000-6 | 400 | 29471 | 50474 | 515.9 | 266.00 | 27.47 | 0.782 | 1.857 |
| Aver. | 400 | 21836 | 43580 | 497.9 | 218.82 | 29.06 | 0.783 | 1.743 |

deformation (P - δ) curve or load-crack mouth opening displacement (P - $CMOD$) curve with a stable descending branch should be obtained. For this purpose, a testing machine under the displacement control is necessary, in addition, the testing machine and the loading devices are demanded for enough stiffness.

According to the principle of work-of-fracture, after taking into account the contribution of tail curve of P_h - $COMD$ on fracture energy, the fracture energy of specimen is calculated from area under the P_h - $COMD$ curve. Because the descending of the tail curve of P_h - $COMD$ is very slow and flat, in addition, because the tail curve can be obtained using some fitting functions, the test can be ended when

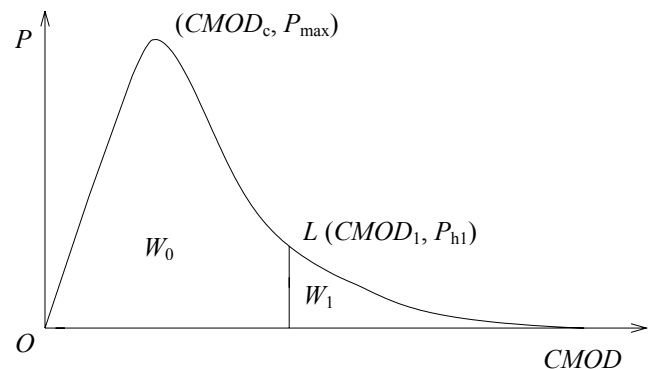


Figure7. The demonstrated plot of fracture energy calculated.

Table3. Fracture energy measured from the experiment.

| Nos. of specimens | m | n | R^2 | $W_1 (N \cdot m)$ | $W_0 (N \cdot m)$ | $\delta_1 (mm)$ | $A_{lig} (mm^2)$ | $G_F=(W_0+W_1)/A_{lig} (N/m)$ |
|-------------------|--------|-------|-------|---------------------|---------------------|-------------------|--------------------|-------------------------------|
| CT200-1 | 8.250 | 4.025 | 0.988 | 0.09 | 3.359 | 0.935 | 0.024 | 144 |
| CT200-2 | 2.669 | 1.808 | 0.976 | 0.23 | 4.082 | 1.377 | 0.024 | 182 |
| CT 200-3 | 5.727 | 3.101 | 0.978 | 0.15 | 3.371 | 1.001 | 0.023 | 151 |
| CT 200-4 | 5.224 | 2.466 | 0.986 | 0.22 | 4.531 | 1.170 | 0.024 | 202 |
| CT 200-6 | 1.455 | 1.382 | 0.976 | 0.37 | 3.998 | 1.208 | 0.023 | 187 |
| CT 300-1 | 11.527 | 3.042 | 0.995 | 0.12 | 6.669 | 1.350 | 0.036 | 187 |
| CT 300-2 | 10.175 | 2.663 | 0.993 | 0.53 | 6.059 | 0.978 | 0.036 | 183 |
| CT 300-3 | 3.916 | 1.477 | 0.983 | 0.40 | 6.866 | 1.711 | 0.035 | 205 |
| CT 300-4 | 1.630 | 0.718 | 0.980 | 0.68 | 8.767 | 2.548 | 0.038 | 252 |
| CT 300-5 | 6.292 | 2.331 | 0.982 | 0.27 | 5.601 | 1.247 | 0.035 | 170 |
| CT 400-2 | 12.020 | 2.085 | 0.992 | 0.10 | 9.446 | 2.229 | 0.050 | 191 |
| CT 400-3 | 36.930 | 2.393 | 0.990 | 1.38 | 8.221 | 1.271 | 0.049 | 198 |
| CT 600-1 | 5.623 | 1.117 | 0.992 | 0.54 | 16.315 | 2.553 | 0.076 | 223 |
| CT 600-2 | 16.122 | 1.508 | 0.988 | 0.24 | 18.954 | 2.935 | 0.080 | 239 |
| CT 600-3 | 6.555 | 1.476 | 0.990 | 0.33 | 13.264 | 2.182 | 0.077 | 176 |
| CT 600-4 | 5.283 | 0.955 | 0.990 | 0.67 | 18.510 | 2.868 | 0.079 | 241 |
| CT 600-6 | 5.463 | 1.177 | 0.991 | 0.52 | 18.487 | 2.388 | 0.078 | 245 |
| CT 800-1 | 5.320 | 0.969 | 0.961 | 0.84 | 21.602 | 2.580 | 0.116 | 194 |
| CT 800-2 | 5.564 | 0.918 | 0.956 | 0.84 | 24.572 | 2.834 | 0.119 | 214 |
| CT 800-3 | 10.075 | 1.143 | 0.991 | 0.66 | 22.327 | 2.811 | 0.113 | 203 |
| CT 800-4 | 10.430 | 1.315 | 0.992 | 0.58 | 20.021 | 2.459 | 0.116 | 178 |
| CT 800-5 | 7.089 | 0.996 | 0.994 | 0.86 | 23.869 | 2.751 | 0.111 | 223 |
| CT 800-6 | 8.001 | 1.185 | 0.995 | 0.69 | 22.316 | 2.453 | 0.111 | 208 |
| CT 1000-1 | 11.327 | 0.922 | 0.994 | 1.56 | 34.365 | 2.920 | 0.159 | 227 |
| CT 1000-2 | 12.588 | 1.329 | 0.982 | 0.96 | 30.363 | 2.190 | 0.158 | 199 |
| CT 1000-3 | 14.549 | 0.939 | 0.992 | 1.77 | 45.203 | 2.972 | 0.166 | 284 |
| CT 1000-4 | 8.869 | 0.853 | 0.983 | 1.53 | 34.096 | 2.978 | 0.159 | 225 |
| CT 1000-5 | 5.764 | 0.662 | 0.977 | 2.27 | 36.604 | 2.973 | 0.157 | 248 |
| CT 1000-6 | 10.632 | 1.174 | 0.993 | 0.99 | 31.506 | 2.417 | 0.165 | 197 |

* The whole curves of P - $CMOD$ of specimens CT400-1&CT400-6 could not be measured because the clip gage dropped out.

the curves tend to zero. The load at the ending point is denoted as P_{h1} , the corresponding crack mouth opening displacement is denoted as $CMOD_1$, so the tested work of fracture W_0 is the area under P_{h1} - $CMOD_1$ curve. According to its tendency, the tail of the curve can be obtained by fitting function, thus the work of fracture given by this part is denoted as W_1 . For example, the developing trend of the tail curves of vertical load-crack mouth opening displacement (P_V - $CMOD$) behind the ending point almost fits to exponential function in the testing range, that is

$$P_V = me^{-n\delta} \quad (1)$$

where δ is the crack mouth opening displacement; m, n are parameters of exponential function. So the work of fracture between the ending point and the real zero point is given by

$$W_1 = \int_{\delta_1}^{\infty} me^{-n\delta} / (2 \tan \theta) d\delta = \frac{m}{ne^{n\delta_1} \cdot 2 \tan \theta} \quad (2)$$

where δ_1 is crack mouth opening displacement at the ending point ($\delta_1=CMOD_1$). Figure 7 shows the plot

of fracture energy calculated. Therefore, the fracture energy G_F according to the RILEM recommendation is given by dividing the total work W (i.e. $W=W_0+W_1$) by the area of the initially uncracked ligament, that is

$$G_F = \frac{W}{A_{lig}} = \frac{W_0 + W_1}{A_{lig}} \quad (3)$$

These are listed in Table3. Fig. 8 shows that the average of the calculated fracture energy G_F remains independent of the specimen height.

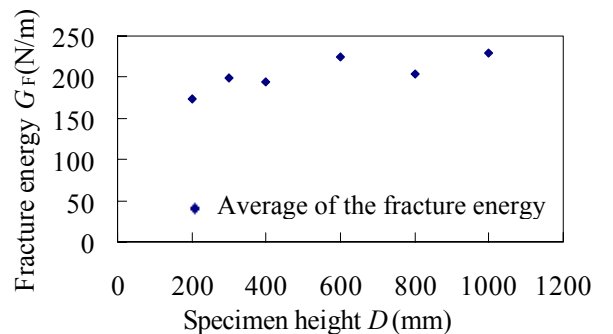


Figure8. The fracture energy vs. specimen height.

Table 3 indicates that the fracture energy measured by the tail curves of the P_h - $CMOD$ after the ending seldom contributed to the total fracture energy, nearly 3.8%. and Fig.7 shows that fracture energy calculated by equation (1)~(3) can be taken as independent of the specimen height within the range

5 CONCLUSION

In this paper, an attempt is made to determine the fracture parameters such as double-K fracture parameters K_{Ic}^{mi} , K_{Ic}^{un} and fracture energy G_F using the wedge-splitting test on compact tension specimen testing method. This new method has the advantages of two traditional methods, that is, wedge-splitting method and compact tension method. It not only may eliminate the influence of the additional moment caused by the non-collinear vertical forces on the true values of fracture parameters, but also may weaken the stiffness requirement often needed for fracturing a specimen. From the studied results, it is shown that wedge-splitting on compact tension specimens fracture testing method is simple and stable, hence having low operation skill. In addition, it has been found that the measured double- K fracture parameters K_{Ic}^{mi} , K_{Ic}^{un} are independent of specimens' size, which further verifies the conclusion that the double- K fracture parameters are the material parameters. In the same way, the calculated fracture energy from the curve of P_h - $CMOD$ after taking into account the contribution of tail curve of P_h - $CMOD$ shows no size-effect within the testing rangsof the discrete property of the concrete, which is consistent with the results that the double- K parameters are independent of the specimen height. It illuminates that the testing error can be eliminated by improving the testing method. In addition, the variation coefficient of the fracture energy is about 0.113, which is higher than the one of fracture toughness, which is maybe due to the random distribution of the aggregate as well as differences between routes of the cracking. However, it can be summarized that the fracture energy G_F can show the behavior of the material without size-effect.

REFERENCES

- ASTM Standard E399-72 1972. *Standard Method of Test for Plane-Strain Fracture Toughness of Metallic Materials*. Annual Book of ASTM Standards.
- B.Hillemeier & H.K.Hilsdorf. Fracture Mechanics Studies on Concrete Compounds. *Cement and Concrete Research*, 1977, 7: 523-536.
- Brühwiler, E. and Wittmann, F.H. 1990. The wedge splitting test, a new method of performing stable fracture mechanics tests. *Engineering Fracture Mechanics* 35(1-3):117-125.
- Hillemeier, B. & Hilsdorf, H.K. 1977. Fracture mechanics studies on concrete compounds. *Cement and Concrete Research* 7(5):523-535.
- Kim, J.K., Mihashi, H., Kirikoshi, K. & Narita, T. 1992. Fracture energy of concrete with different specimen size and strength by wedge splitting test. *Fracture Mechanics of Concrete Structures* (Edited by Bazant). Elsevier Applied Science, London and New York: 561-566.
- Mihashi, H., Nomura, N. & Kim, J.K. 1994. Fracture mechanics properties and size effect in concrete. *Size-Scale Effects in the Failure Mechanisms of Materials and Structures*. E & FN Spon: 399-410.
- Ratanalert & Wecharatana, M. 1989. Evaluation of fictitious crack and two-parameter fracture models. *Fracture Toughness and Fracture Energy* (Edited by Mihashi et al.). Balkema, Rotterdam:345-366.
- Swartz, S.E. & Refai, T.M.E. 1987. Influence of Size on Opening Mode Fracture Parameters for Precracked Concrete Beams in Bending. Proceedings of SEM-RILEM International Conference on Fracture of Concrete and Rock (Edited by S.P. Shah and S.E. Swartz). Houston, Texas:242-254.
- Wang and Wu, K. 1992. Fracture parameters of concrete as determined by means of wedge splitting test. *Fracture Mechanics of Concrete Structures* (Edited by Bazant), Elsevier Applied Science, London and New York: 461-464.
- Wittmann, F.H., Mihashi, H. & Nomura, N. 1990. Size effect on fracture energy of concrete. *Engineering Fracture Mechanics* 35(1-3): 107-115.
- Xu, Shilang & Reinhardt, H.W. 1999a. Determination of double- K criterion for crack propagation in quasibrittle materials, part I: experimental investigation of crack propagation. *International Journal of Fracture* 98(2): 111-149.
- Xu, Shilang & Reinhardt, H.W. 1999b. Determination of double- K criterion for crack propagation in quasibrittle materials, part II: analytical evaluating and practical measuring methods for three-point bending notched beams. *International Journal of Fracture* 98(2), 151-177.
- Xu, Shilang & Reinhardt, H.W. 1999c. Determination of double- K criterion for crack propagation in quasibrittle materials, part III: compact tension specimens and wedge splitting specimens. *International Journal of Fracture* 98(2), 179-193.
- Xu, S. & Zhao, G. 1991. Concrete fracture toughness of huge specimens and criterion of fracture toughness for judging cracks in high concrete dam. *China Civil Engineering Journal* 24(2): 1-9.
- Xu, S., Zhao, G., Huang, C., Liu, Y., Jin, G. & Wang, F. 1991. Fracture energy and strain field near the tip of a notch in huge concrete specimen under compact tension. *Journal of Hydraulic Engineering* 11: 17-25.
- Zhao, G., Jiao, H. & Xu, S. 1991. Study on fracture behavior with wedge splitting test method. *Fracture Processes in Concrete, Rock and Ceramics* (Edited by van Mier et al.). E & F.N. Spon, London: 789-798.
- Zhu, X. 1997. Transport organischer Flüssigkeiten in Betonbauteilen mit Mikround Biegerissen. Deutscher Ausschuss für Stahlbeton, Heft 475, Beuth Verlag GmbH, Berlin, S: 1-104.